analytical chemistry

Article

pubs.acs.org/ac

Quantification of Peptide *m/z* Distributions from ^{13}C-Labeled Cultures with High-Resolution Mass Spectrometry

Doug K. Allen,*[,†,∥] Joshua Goldford,[‡] James K. Gierse,[†] Dominic Mandy,[‡] Christine Diepenbrock,[†,§] and Igor G. L. Libourel*[,‡,∥]

[†]Plant Genetic Research Unit, Agricultural Research Service, U.S. Department of Agriculture (USDA-ARS), Donald Danforth Plant Science Center, 975 North Warson Road, St. Louis, Missouri 63132, United States

[‡]Department of Plant Biology, University of Minnesota, 1500 Gortner Avenue, Saint Paul, Minnesota 55108, United States

Supporting Information

ABSTRACT: Isotopic labeling studies of primary metabolism frequently utilize GC/MS to quantify ^{13}C in protein-hydrolyzed amino acids. During processing some amino acids are degraded, which reduces the size of the measurement set. The advent of high-resolution mass spectrometers provides a tool to assess molecular masses of peptides with great precision and accuracy and computationally infer information about labeling in amino acids. Amino acids that are isotopically labeled during metabolism result in labeled peptides that contain spatial and temporal information that is associated with the biosynthetic origin of the protein. The quantification of isotopic labeling in peptides can therefore provide an assessment of amino acid metabolism that is specific to subcellular, cellular, or temporal conditions. A high-resolution orbital trap was used to quantify isotope labeling in peptides that were obtained from unlabeled and isotopically labeled soybean embryos and *Escherichia coli* cultures. Standard deviations were determined by estimating the multinomial variance associated with each element of the *m/z* distribution. Using the estimated variance, quantification of the *m/z* distribution across multiple scans was achieved by a nonlinear fitting approach. Observed *m/z* distributions of uniformly labeled *E. coli* peptides indicated no significant differences between observed and simulated *m/z* distributions. Alternatively, amino acid *m/z* distributions obtained from GC/MS were convolved to simulate peptide *m/z* distributions but resulted in distinct profiles due to the production of protein prior to isotopic labeling. The results indicate that peptide mass isotopologue measurements faithfully represent mass distributions, are suitable for quantification of isotope-labeling-based studies, and provide additional information over existing methods.

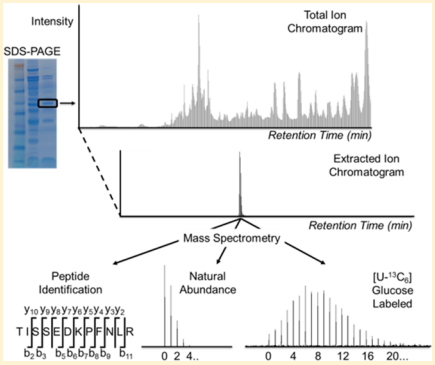

Eukaryotic metabolism occurs within tissues and organelles and is therefore highly organized at both cellular and subcellular levels. Along with temporal developmental queues, the spatial architecture complicates experiments in cell biology. Nonetheless, genetic engineering relies on knowledge of cellular location and timing for the design of transit peptides and promoter sequences. The importance of properly selective targeting in plants is well-known and includes dramatic examples such as increased levels of carotenoid production by 50-fold[1] and leaves that produce a significant percentage of total dry weight as polyhydroxybutrate.[2] Metabolic studies often lack subcellular and temporal detail, resulting in a disconnect between the ability to generate active enzymes transgenically and foreseeing their impact on metabolic network function.

Metabolic flux analysis (MFA) based on isotopic labeling provides a description of cellular operation to aid engineering and can indicate unconventional pathway use in plants (reviewed in refs 3−6), but frequently flux maps are not extensively resolved at the subcellular level. Obtaining information specific to compartments in eukaryotes is experimentally challenging and limits quantitative cellular descriptions.[7−18] Recently we reported an approach to investigate the labeling in protein subunits that are made in different locations.[19] Proteins in plants are translated from one of three genomes located in the chloroplast, nucleus, or mitochondria. Peptide translation utilizes amino acid pools specific to a particular organelle, and therefore, ^{13}C-labeling analysis can detect the subcellular biosynthesis on the basis of differences in enrichment. For example, the large and small subunits of RuBisCO were compared after culturing *Brassica napus* embryos in ^{13}C medium. Disparities in isotopic labeling indicated that amino acids were made in different locations, but the sensitivity of GC/MS and losses in protein and amino acids during processing limited this approach to abundant, relatively pure proteins that meet steady-state labeling criteria.

Given the challenges associated with obtaining reliable amino acid labeling information for proteins present at low abundance, we developed LC−MS/MS-linked orbital ion trap (LC-ESI-LTQ-Orbitrap Velos, ThermoElectron; referred to hereafter as

Received: December 9, 2013
Accepted: January 3, 2014
Published: January 3, 2014

   dx.doi.org/10.1021/ac403985w | *Anal. Chem.* 2014, 86, 1894−1901

"orbital trap") techniques to accurately measure labeling in peptides. Peptide enrichment can be subsequently used to infer labeling in amino acids when deconvolved through metabolic flux analysis.[20] The direct measurement of peptides has several benefits relative to traditional assessments of labeling in protein-hydrolyzed amino acids. First, proteins from biomass can be processed with limited or no purification. Protein sequence identification is genome-specific and can be linked with cell type or subcellular location and therefore does not depend upon the isolation purity of the protein. In fact, potentially many proteins from different locations could be simultaneously analyzed in a single experiment. Furthermore, peptides can provide labeling information on up to all 20 amino acids because hydrolysis steps that degrade amino acids are avoided. Given that GC/MS methods usually do not report tryptophan or cysteine due to oxidative degradation, asparagine or glutamine due to deamidation, arginine due to complex cracking patterns, and other amino acids including histidine, lysine, and methionine that are not always present in sufficient amounts for analyses, an alternative sensitive method that provides additional information is desired for metabolic studies.

High-resolution MS instruments can quantify proteins and measure peptide masses with parts per million accuracy[21] and attomolar sensitivities.[22] Quantification methods including SILAC (stable isotope labeling with amino acids)[23,24] and iTRAQ (isobaric tags for relative and absolute quantitation),[25] and their derivatives[26−28] rely on isotopic labeling to distinguish proteins on the basis of mass (reviewed in refs 29−32). Proteomic investigations have also used isotopes to evaluate protein turnover[33−35] and altered protein production[36−38] and to qualitatively inspect amino acids.[39] Recent metabolite studies have focused on distinguishing elemental isotopes[40] and enhanced small molecule identification,[41−43] but these methods have not aimed to accurately quantify large m/z envelopes that accompany isotopic labeling in peptides, which is the focus of this study.

Labeled protein was obtained from *Escherichia coli* grown with 7% uniformly labeled glucose or from developing soybeans cultured with [U-$^{13}C_6$]glucose. The instrument resolution, sensitivity, variation in scans, dynamic range, and accuracy were all probed. Peptide characteristics including the charge state, oxidation number, and peptide lengths established through proteolysis were also evaluated. In single scans, peptide m/z distributions were converted to absolute ion estimates, which made it possible to associate a multinomial variance with each element of the m/z distribution. With the estimated variance, m/z distributions were quantified across multiple scans using a nonlinear fitting approach. The observed isotopologues from uniformly labeled *E. coli* peptides indicated no significant differences between observed and simulated m/z distributions. The same protein was hydrolyzed, and isotopic labeling in amino acids was quantified with GC/MS. The amino acid measurements were subsequently convolved and compared with those obtained directly from the orbital trap. Isotopically labeled amino acids measured by GC/MS resulted in simulated peptides that were distinct from those directly measured with the orbital trap.

EXPERIMENTAL SECTION

Chemicals. [U-$^{13}C_6$]Glucose, sucrose, glucose, glutamine, asparagine, plant protease inhibitor cocktail, Ponceau-S, bovine serum albumin (BSA), trypsin, chymotrypsin, thermolysin, proteinase K, and all common buffer reagents were obtained from Sigma (St. Louis, MO). Sodium dodecyl sulfate−polyacrylamide gel electrophoresis (SDS−PAGE) reagents were purchased from Life Technologies Inc. (Carlsbad, CA), and derivatization reagent *N*-methyl-*N*-(*tert*-butyldimethylsilyl)trifluoroacetamide (MTBSTFA) + 1% *tert*-butyldimethylchlorosilane (TBDMCS) was purchased from Thermo Scientific (Waltham, MA).

***E. coli* Culture.** *E. coli* strain G1655CGSC was cultured at 37 °C with vigorous shaking in M9 medium containing 0.4% unlabeled glucose or glucose uniformly labeled with 7% ^{13}C. To ensure that all newly synthesized protein was made from labeled glucose, 100 mL of medium was inoculated with 1 mL of starting culture and grown to an OD600 of 1.0. A 10 mL volume of this culture was transferred to 900 mL of medium and grown to an OD600 of 1.2. Cells were harvested by centrifugation at 14 000 rpm for 20 min and stored at −80 °C until use.

Soy Embryo Culture. *Glycine max* (cv. Jack) was grown in greenhouse conditions, which included a 14 h/10 h light/dark cycle, daily watering, and fertilization. Green soybean pods were harvested, immediately placed on ice, and sterilized with 5% bleach followed by sterile H_2O. Embryos of 25−40 mg (fresh weight) were excised under sterile conditions. Embryos were placed in a 250 mL flask containing 15 mL of culture medium: 150 mM sucrose, 75 mM glucose, 45 mM glutamine, 16 mM asparagine, 5 mM MES, pH 5.7, with KOH.[44] Trace salts and vitamins[45,46] were added, and the medium was filter sterilized. For labeling experiments [U-$^{13}C_6$]glucose was exchanged for unlabeled glucose. Embryos were grown for two weeks in a humidified incubator with constant 30 μmol of photons m^{-2} s^{-1} at 27 °C.

Protein Isolation. Total soluble protein was isolated from *E. coli* as described in the Supporting Information (Experimental Methods). Briefly, cells cultured in M9 medium were isolated, and subsequently DNA was precipitated with ammonium sulfate. Protein was further purified by dialysis and Q-Sepharose (Sigma) before equilibration in 50 mM ammonium bicarbonate and stored at −80 °C. Soy embryos were homogenized, and protein was isolated using 50 mM HEPES buffer. SDS−PAGE samples were prepared by boiling several milligrams of protein in sample buffer and running it on 4−12% Nu-PAGE gel at constant voltage (200 V) for 35 min, and for amino acid analysis the proteins were transferred onto Immobilon-P, poly(vinylidene fluoride) (PVDF) paper by electroblot for 2 h at 200 mA constant current (Supporting Experimental Methods).

Amino Acid Hydrolysis and Analysis by GC/MS. Soybean storage proteins excised from PVDF were hydrolyzed with 6 N HCl at 110 °C for 48 h, dried, and converted to *tert*-butyldimethylsilyl derivatives. Amino acids were suspended in acetonitrile plus MTBSTFA for 30 min at room temperature followed by 100 °C for 2 h. Amino acid isotopologues were analyzed by an ISQ GC/MS instrument (Thermo Scientific, Waltham, MA) operating in selected ion monitoring mode (SIM) with a DB-5 column (30 × 0.25 mm i.d., Restek, Bellefonte, PA) using a ramp profile of 100 °C for 4 min, then 100−200 °C at 4 °C/min, and then 200−300 °C at 10 °C/min with a helium carrier gas flow rate of 1.2 mL/min. Injection, mass spectrometer transfer line, and ion source temperatures were 230, 250, and 250 °C, respectively. Samples were run in triplicate.

Trypsin Digest and Peptide Preparation. Excised SDS−PAGE bands were destained with 50% acetonitrile and 100 mM

dx.doi.org/10.1021/ac403985w | *Anal. Chem.* 2014, 86, 1894−1901

ammonium bicarbonate for several hours, then reduced with 10 mM DTT, and alkylated with iodoacetamide (55 mM in 100 mM ammonium bicarbonate) at room temperature. After being washed with ammonium bicarbonate and acetonitrile, the protein was dried and trypsin digested as described in the Supporting Information (Experimental Methods). The peptides were suspended in 5% acetonitrile, 0.1% formic acid prior to mass spectrometry.

Orbital Trap Velos Mass Spectrometry. Peptides were analyzed by LC−MS/MS using a nano-LC 2D (Eksigent, Dublin, CA) coupled to an LTQ-Orbitrap Velos (Thermo Fisher Scientific, San Jose, CA). The instrument contained a trap column (C18 PepMap100, 300 μm × 1 mm, 5 μm, 100 Å, Thermo Fisher Scientific) followed by an analytical column (Acclaim PepMap C18, 15 cm × 75 μm × 3 μm, 100 Å, Thermo Fisher Scientific) through which peptides were eluted at a rate of 260 nL/min. The gradient changed from 98% buffer A (0.1% formic acid)/2% buffer B (0.1% formic acid in 100% acetonitrile) after a 2 min hold period to 40% buffer B in 83 min, followed by an increase to 2% buffer A/98% buffer B in 5 min and was held for an additional 2 min. The mass spectrometer was operated in positive ionization mode, and survey scans were performed in the FT cell in the range of 300−2000 m/z with the resolution set to 30−60000 at 400 m/z with additional operational parameters described in the Supporting Information (Experimental Methods).

The Mascot Daemon v2.4 (Matrix Science) data processing software with the NCBI database was used to evaluate the peptides. The search parameters were as follows: trypsin-based cleavage, two missed cleavage sites allowed, and methionine oxidation allowed. The mass error tolerance for precursor ions was set to 15 ppm and 0.08 Da for fragment ions. Scaffold (version Scaffold_3.3.1, Proteome Software Inc., Portland, OR) was used to validate MS/MS-based peptide and protein identifications.[47] Peptide identifications were accepted if they could be established at greater than 80.0% probability as specified by the Peptide Prophet algorithm.[48] m/z values were converted to molecular mases by accounting for the charge states.

RESULTS AND DISCUSSION

Biomass Production and Culturing Conditions for Steady-State Isotopic Labeling of Proteins. *E. coli* was cultured in minimal M9 medium at 37 °C with or without ^{13}C isotopes of glucose (~7% uniformly labeled glucose, NMR; Table S-1, Supporting Information). Each culture was twice diluted into fresh medium during growth to eliminate unlabeled biomass. Glucose was the sole source of organic carbon provided to *E. coli*, and each culture resulted in approximately 4 g of fresh weight biomass/L of culture. Soybeans (*G. max* cv. Jack) were grown in greenhouses maintained at approximately 23−30 °C with 14 h of daylight consistent with growth conditions in St. Louis, MO. Immature pods were harvested and aseptically dissected, and embryos were cultured with carbon and nitrogen sources to mimic *in planta* development as previously described.[45,46,49] During a two week period of steady-state labeling, the embryos accumulated 7.1 mg of dry weight per day, amounting to approximately 4.1 doublings in the embryo biomass, which is equivalent to 94% of the total biomass produced. Embryos were also cultured with [U-$^{13}C_6$]-glucose to provide a source of nonuniformly labeled peptides. *E. coli* labeled protein and labeled and unlabeled soybean biomass served as standards for method development.

Evaluation of Peptides for LC−MS/MS Peptide-Based Labeling Analysis. Soybeans are approximately 40% protein by weight and contain two major storage proteins, β-conglycinin and glycinin.[50] Cultured embryos were harvested by centrifugation and processed as a crude preparation or with subunit isolation by SDS−PAGE. Protein subunits were digested with trypsin with or without prior reduction and alkylation. Other proteases that produce small peptides were less reliable and produced a limited number of peptides (Table S-2, Supporting Information); however, further optimization of different cleavages could benefit focused studies by providing additional peptide labeling descriptions. The orbital trap was used to generate full scans that were analyzed with protein assembly software (see the Experimental Section). Three SDS−PAGE bands representing different subunits of β-conglycinin were examined with the orbital trap (Table S-3, Supporting Information). The amino acid sequence and trypsin digestion pattern were used to calculate the expected number of cleavages and the number of predicted peptides. Identified and quantified peptides are described in Table S-4 (Supporting Information) and reflect the peptide set that met the 95% quality score/confidence threshold setting. Peptides greater than 35 amino acids exceeded the range of monitored masses. GC/MS labeling in amino acids of different subunits is summarized in Table S-5 (Supporting Information). The labeling differences in the three storage protein subunits were modest, and further quantification efforts of soybean protein focused on the β-conglycinin subunit that gave the greatest number of identified peptides (Table S-3). The ion chromatograms for each peptide were identified using product ion fragmentation patterns and protein assembly software. Intensities were manually extracted to quantify the m/z intensity distributions for both unlabeled and labeled peptides. A schematic overview of the process is presented in Figure 1. Note that for simplicity the increasing m/z has been indexed; for example, $(m + 5)/z$ is subsequently referenced as "5", and the monoisotopic m/z is equivalent to 0.

Details of the LC−MS/MS parameters are provided in the Experimental Section. The m/z distributions of 53 unlabeled abundant peptides were quantified from a list generated by the protein assembly software. The unlabeled peptides were compared to simulated m/z distributions generated from reported natural abundance levels[51] and chemical composition. Each carbon in naturally abundant peptides has an identical probability of ^{13}C labeling. The same holds true for the isotopes of all other elements, and we simulated peptide mass distributions by successively convolving the mass distributions of all constituent elements (i.e., carbon and heteroatoms). The measured and simulated fractional abundances were similar (Figure 2) and indicated good agreement across abundances ranging over several orders of magnitude (Table S-6, Supporting Information). Peptide charge did not impact label quantification as indicated by a subset of 13 peptides measured with charge states of both 2 and 3. Oxidized and nonoxidized forms of peptides that contained methionine were also similar, indicating good technical agreement (Figure 2); however, the m/z separation of oxidized/nonoxidized peptides is small (i.e., 16 Da), and we investigated if this could reduce the isotopic envelope width that we could quantify.

Given that sulfur-containing amino acids are often present at lower concentrations in some plant tissues and that they can be degraded during protein hydrolysis (i.e., cysteine), they are frequently not reported; however, we further evaluated the presence of cysteine and methionine in peptides identified by

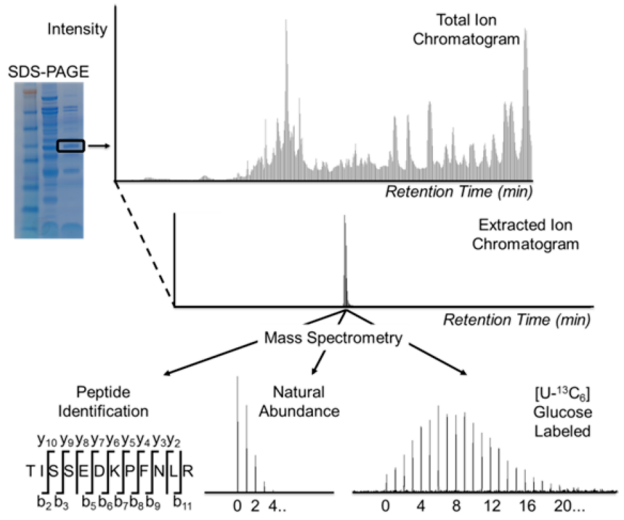

Figure 1. Process for peptide evaluation by LC–MS/MS with the orbital ion trap. Soybean or *E. coli* protein that is ^{13}C-labeled through culturing was purified and separated by SDS–PAGE. Individual bands were reduced, alkylated, and digested with trypsin prior to inspection by mass spectrometry. Individual m/z values from peptides containing natural abundance levels of isotopes were used with protein assembly software to identify peptide sequences and retention times. ^{13}C-enriched proteins were similarly processed, and peptides were analyzed for labeling.

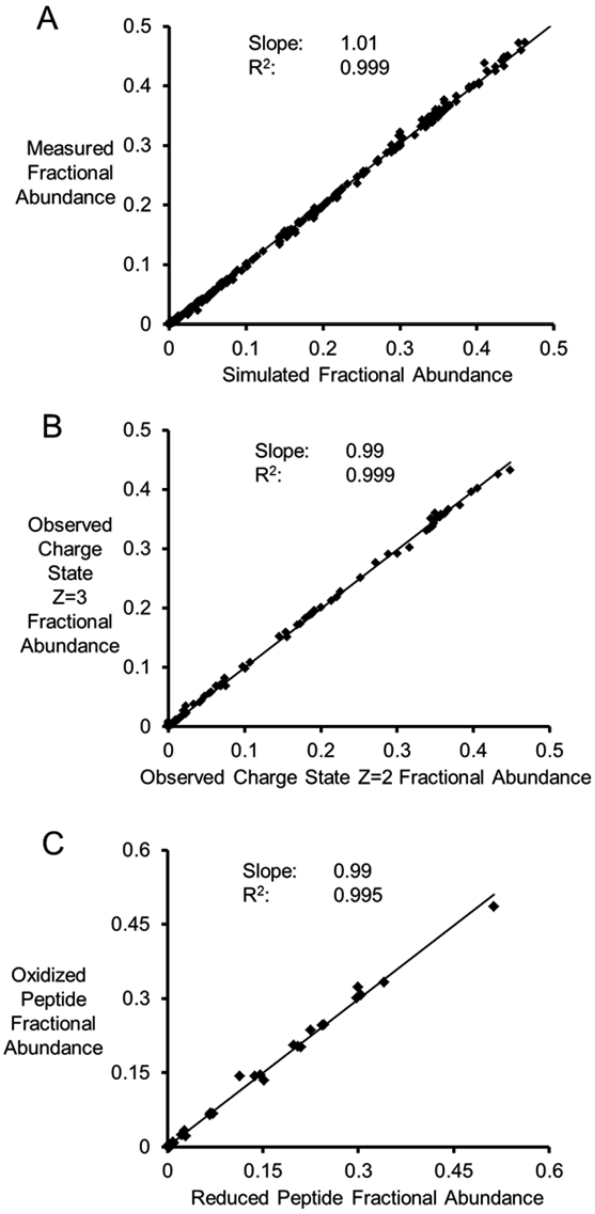

Figure 2. Technical comparison of direct orbital trap peptide fractional abundances to simulated measurements of natural abundance. (A) Comparison of 53 peptides reveals a strong linear relation at all relative abundances. (B) A subset of 13 peptides were present at multiple charge states. The fractional abundances were not affected by the charge. (C) Similarly, the presence of methionine and oxidized methionine did not impact the fractional abundance quantification.

protein assembly software. In all instances cysteine residues were carboxymethylated (Table S-7a, Supporting Information), reflecting the quantitative reduction and alkylation by dithiothreitol and iodoacetamide.[52] The analysis of methionine-containing peptides (Table S-7b and associated description) indicated that oxidized peptides do not coelute with nonoxidized forms. The difference in retention times usually approached 1 min or more and allowed for completely independent inspection of m/z values (Table S-7b). In summary, the analysis of both soybean protein and *E. coli* biomass indicated (i) cysteine residues are quantitatively reduced and alkylated so that only the reduced forms were observed in peptides (Table S-7a) and (ii) peptides containing methionine or oxidized methionine were chromatographically resolved (Table S-7b); therefore, cysteine- and methionine-containing isotopologues can be quantified without concern. Additionally, mass resolution did not markedly alter the number of measurable elements of the m/z distributions or the average labeling description (Table S-8, Supporting Information).

Quantification of Orbital Trap Mass Distributions. To optimize the quality of the m/z quantification, m/z intensity distributions over a range of scans were included. Due to the incidental absence of lower intensity m/z elements from the distribution, simple integration of intensities over several scans results in overestimations of abundant elements. By scaling intensity values to the base peak of each scan, good quantification can be achieved, but the precision is still compromised by the contribution of both the variation of the base peak and the variation in the m/z values that are scaled. The significance of this effect is inversely proportional to the relative intensity of the base peak, and because the base peak will have only a modest intensity in significantly labeled peptides, a better approach is to normalize by the sum of all m/z elements. This requires all m/z elements to be present in all scans, yet missing values in orbital trap spectra is common for signals that are close to the limit of detection (Figure 3) and also occurs sporadically for peaks with significant intensities.[53] To overcome this limitation, the m/z distribution and the total peptide intensities of each scan were fitted to the observed m/z measurements. The optimization problem was nonlinear due to the multiplication of the total ion intensity parameters of each scan with the elements of the m/z distribution. This gap-filling procedure was overdetermined and solved with the Matlab optimization function "fmincon".

Estimation of Orbital Trap Measurement Standard Deviations. The total population of peptide molecules was assumed to be significantly larger than the population observed

dx.doi.org/10.1021/ac403985w | *Anal. Chem.* 2014, 86, 1894–1901

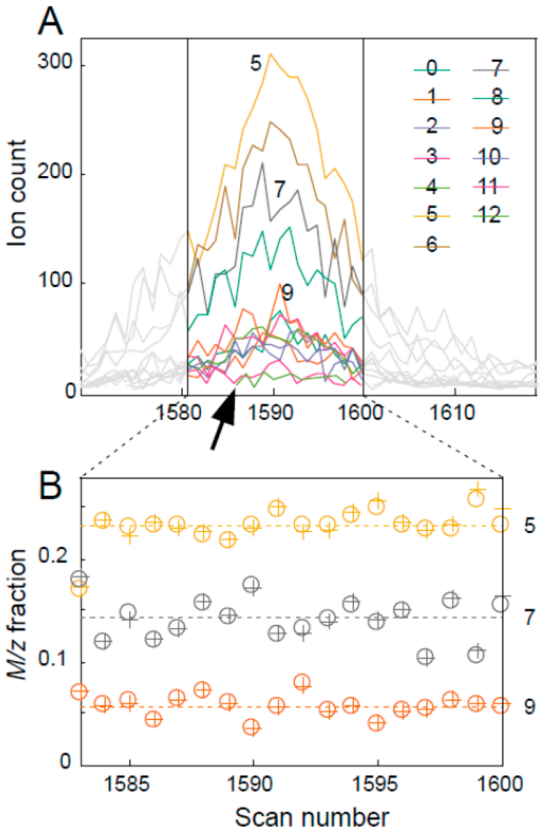

Figure 3. Extracted ion chromatograms (EICs) of peptide VLFSR from ^{13}C-labeled soybeans. (A) EICs are colored for scans within the full width at half-height of the total extracted isotopologue chromatogram, which was used for quantification. The EIC of mass trace 12 (monoisotopic m/z + 12/z) was only present in a subset of the scans (arrow). (B) Quantification of the EICs: 5, 7, and 9 are presented with scaling to the base m/z peak (+) or through nonlinear fitting (○). The dotted line indicates the mean fractional abundances.

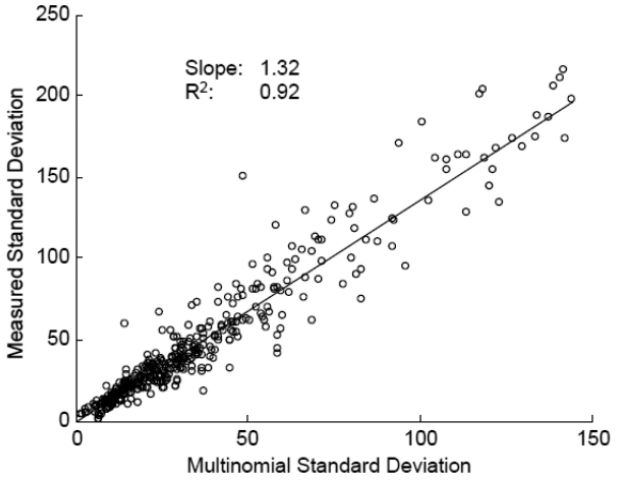

Figure 4. Observed standard deviations as a function of the multinomial sampling standard deviation. The multinomial sampling error closely approximated (correlation coefficient R^2 of 0.92) and was linearly related (slope of 1.32) to the empirically determined standard deviations. This relationship was used to infer standard deviations for ion intensity measurements from the calculated multinomial sampling error.

by the orbital trap, so that the measurements could be modeled as a multinomial distribution that was sampled with replacement. The orbital trap signal was converted into ion counts by substituting raw signal-to-noise values using the following approximate relationship:[54] $I_i = S_iK(R/R_0)^{1/2}/N_iz_i$, where S_i/N_i is the signal-to-noise ratio, K is the noise band, z_i is the charge, R is the acquisition resolution, and R_0 is the reference resolution. Each m/z distribution contains a discrete number of elements q (m/z values), and each sampling event results in drawing an m/z element. The total number of ions of a peptide in the orbital trap in a scan establishes the sample size, n, where $n = \sum_{i=0}^{q} I_i$, and the fraction of each m/z element (i) relative to all m/z isotopologues is given by p_i. The multinomial sample mean and variance for each m/z element are np_i and $np_i(1 - p_i)$, respectively. It follows that the variance of the multinomial distribution scales with the signal intensity (linear with n) and that the standard deviation scales with the root of the signal intensity. The standard deviations for the m/z measurements were computed from the multinomial variance. For comparison, the standard deviations were also determined empirically from the residuals of the scans (Figure 4). The relationship between the standard deviations expected from the multinomial sampling and the observed standard deviations was highly correlated (R^2 = 0.92). The standard deviations that were calculated from the multinomial probability were smaller than the measured values (slope of 1.32), but scaled linearly. The slope value >1 indicated that the calculated ion count consistently overestimated the actual ion count and therefore underestimated the associated standard deviations. Because approximately 30 independent measurements are required to reliably estimate standard deviations, the multinomial standard deviations determined were used in combination with the observed regression relationship (Figure 4) to estimate more precise standard deviations.

Quantitative Validation of Mass Distributions. To quantitatively test if orbital trap m/z distributions faithfully represented the relative ion abundances of peptides, observed ion abundances were compared to simulated mass distributions through χ^2 evaluation. The residuum for the χ^2 test was $\sum_{ij} n_j(mf_{ij} - p_{ij})^2/p_{ij}(1 - p_{ij})$, where n_j was the total ion count of peptide j. First the natural abundances of isotopes in proteins were measured and compared to simulated distributions (Figure 5A). In a naturally abundant sample each carbon in a peptide has an identical probability of being ^{13}C; therefore, peptide mass distributions can be predicted by successively convolving the isotopic mass distributions of all constituent atoms, carbons and heteroatoms alike. A larger range of m/z elements was considered through the evaluation of 7% uniformly labeled protein (Figure 5B). The mean carbon atom percent enrichment for the 7% labeled protein was calculated from the MS data prior to generation of the simulated peptide mass distributions (Table S-9, Supporting Information), and the labeling in fed glucose was verified using NMR (Table S-1, Supporting Information). The 7% *E. coli* labeled peptides passed the χ^2 test, indicating that they were not significantly different from the simulated distributions (p > 0.05), whereas the predicted m/z distribution for natural abundance was statistically different from the measured values. The discrepancy between the results for the 7% labeled and naturally abundant peptide sets may be due to the lower relative intensities of the m/z elements in the 7% spectra (i.e., the peptide signal is spread over more m/z elements). The lower intensities reduced the difference between predicted and observed values (relative to the associated standard deviations) so that the differences may not have been statistically

dx.doi.org/10.1021/ac403985w | *Anal. Chem.* 2014, 86, 1894−1901

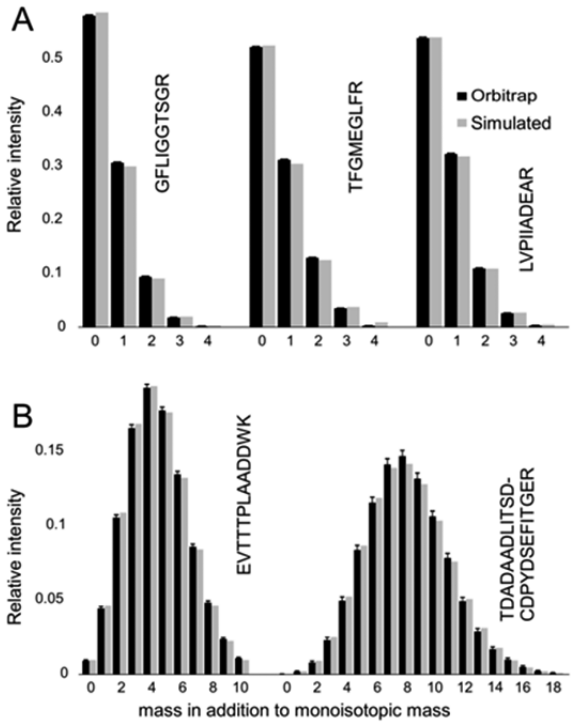

Figure 5. Comparison of peptide labeling. Peptides containing naturally abundant levels of isotopes (A) or those uniformly labeled by culturing *E. coli* (B) were measured by orbital trap (black bars) and compared to simulated mass distributions (gray bars). The estimated standard deviations are represented on the simulated data. Due to strong signal intensity of the selected natural abundant peptides, the standard deviations on the simulated data are barely visible. The m/z values are indexed similarly to those in Figure 3 (e.g., an index of 10 represents the monoisotopic $m/z + 10/z$).

significant. We further investigated if the orbital trap distribution contained a sensitivity bias toward lower or higher m/z values by inspecting the residuals of the combined m/z distributions (Figure 6). The 7% labeled peptides were aligned by their mean mass values so that the x-coordinate in Figure 6 represented the difference between the m/z under consideration and the mean m/z for that entire peptide envelope. For each m/z element the simulated ion count was compared to the measured value and plotted as a relative error (simulated − measured)/measured. The correlation coefficient for the residuals of the 7% labeled distribution was 0.00319, which was not significant (p = 0.3056). The residuals showed some structure, which suggested that the strongest intensities may be slightly overestimated.

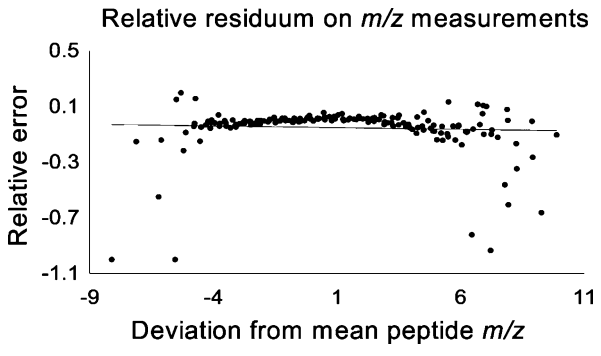

Figure 6. Relative accuracy of m/z intensities. Possible m/z-dependent intensity bias of by the orbital trap measurements was assessed on the 7% labeled peptide set. The mean mass for each isotopologue envelope was determined and assigned a mass deviation of zero. Each intensity was compared to the expected (simulated) value, with the difference between the two scaled by the peak size. The relative errors were plotted against the centered mass deviations for each m/z value (m/z − mean peptide m/z). The plotted trend line suggested no mass-dependent bias, and the R^2 value was not significant.

Comparison of Orbital Trap Measurements to Convolved GC/MS Measurements. To evaluate how orbital trap peptide mass estimates compare to GC/MS-determined amino acid mass distribution measurements, amino acid mass distributions were convolved to simulate peptides (Figure 7).

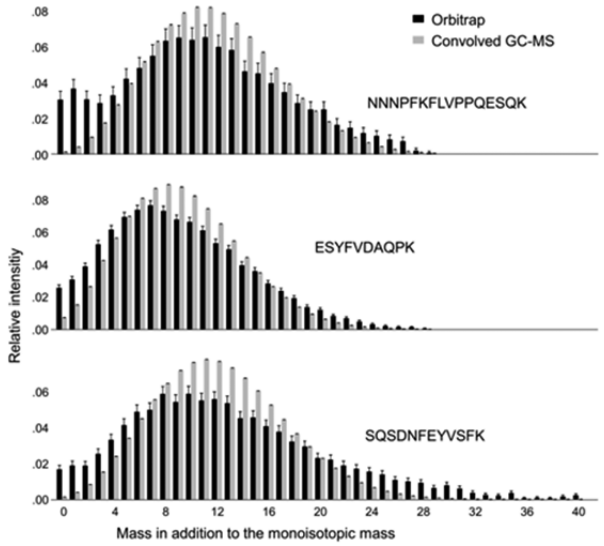

Figure 7. Comparison of convolved GC/MS amino acid measurements to labeled peptide measurements determined by orbital trap. Three peptides obtained from soybean embryos cultured in [^{13}C]-glucose are presented. The convolved GC/MS data (gray bars) fail to faithfully describe two time points in metabolic development: growth on the plant and growth in culture. The separate biological processes result in two peptide descriptions that are overlapping but bimodal as most clearly indicated in the first peptide comparison. Direct measurement of peptides by orbital trap maintains the distinction between the two distributions (black bars). The m/z values are indexed as in Figure 5.

First, GC/MS amino acid measurement methods were extended to include the entire carbon backbone for each amino acid, and the accuracy of the fragments was considered by inspection of natural abundance (Table S-10, Supporting Information). Protein labeled with [U-$^{13}C_6$]glucose was extracted from soybeans and measured by orbital trap as well as hydrolyzed, derivatized, and measured by GC/MS (Table S-11, Supporting Information). The GC/MS values were convolved to simulate peptides for comparison to orbital trap data. Although the mean mass estimates for the distributions were often similar, the simulated distributions from GC/MS data did not match the orbital trap data. The disparity was interpreted to be due to unlabeled peptides present at the start of the culturing period. The unlabeled material is visible in the lower mass range of peptides (Figure 7). Because the GC/MS data were not separated into a naturally abundant and labeled population of amino acids, the convolution of the amino acid distributions was in fact the convolution of the summed amino acid distributions, whereas the orbital trap data represented the

dx.doi.org/10.1021/ac403985w | *Anal. Chem.* 2014, 86, 1894−1901

summed peptide distributions. Consequently, the GC/MS measurements overestimate the center masses of the peptide distribution and underestimate the extreme masses, both the low and high masses. To compare the precision of both technologies, 1000 Monte Carlo samplings of the GC/MS mass estimates were convolved using the 1% technical error associated with the GC/MS measurements as the standard deviation. The standard deviations associated with the orbital trap distributions were estimated using multinomial sampling as before (Figure 7). The simulation suggested that GC/MS distribution estimates can be expected to be very precise, but less accurate. This has important implications for ^{13}C metabolic flux analysis. The significant presence of a naturally abundant protein fraction has been recognized before and is fitted in some flux analysis studies.[55,56]

CONCLUSIONS

This work affirmed the quantification capabilities of high-resolution orbital trap mass spectrometers. The relative peptide m/z intensity distributions closely matched simulated distributions for the investigated conditions. m/z distributions were carefully quantified in such a fashion that missing orbital trap data did not bias the quantification. To establish precise estimates of standard deviations on the orbital trap measurements, the raw signal-to-noise data were converted into absolute ion counts. The multinomial sample standard deviation mapped well to the empirically observed standard deviation, and this relationship was exploited to improve estimates of standard deviations for individual measurements. The developed quantification technology was used to test if the observed m/z values differed significantly from the simulated distributions. Although naturally abundant peptides did differ statistically from the simulated distribution, the differences were very small. m/z distributions of 7% uniformly labeled peptides did not differ significantly from the simulated distributions, and relative intensities within peptides revealed no significant mass bias. Overall, the results indicate that the orbital trap measured m/z distributions were faithful, unbiased representations of the true peptide mass distributions. Compared to peptides generated by convolving GC/MS-derived measurements, peptide-based data have the distinct advantage of encoding the spatial and temporal information associated with the protein from which they were derived. In addition, the unlabeled (original) peptide fraction can be readily recognized, which has the potential to improve flux estimation and to be used for simultaneous protein turnover measurements.

ASSOCIATED CONTENT

Supporting Information

Table S-1, [^{13}C]glucose positional enrichment by NMR, Table S-2, comparison of protease fragmentation, Table S-3, soybean protein subunit description, Table S-4, analyzed peptide description, Table S-5, average amino acid labeling in soybean subunits, Table S-6, comparison of measured natural abundance in peptides to simulated values, Table S-7, peptides containing sulfur-based amino acids, Table S-8, effect of mass spectrometer resolution, Table S-9, *E. coli* peptides generated from culturing with 7% uniformly labeled glucose, Table S-10, average labeling of TBS-amino acid derivatives, Table S-11, amino acid labeling from GC/MS, and supporting experimental methods. This material is available free of charge via the Internet at http://pubs.acs.org.

AUTHOR INFORMATION

Corresponding Authors

*E-mail: Doug.Allen@ars.usda.gov. Fax: 314-587-1560.
*E-mail: Libourel@umn.edu. Fax: 612-624-6264.

Present Address

[§]C.D.: Department of Plant Breeding and Genetics, Cornell University, Ithaca, NY 14853, United States.

Author Contributions

[‖]D.K.A. and I.G.L.L. contributed equally to this work.

Notes

The authors declare no competing financial interest.

ACKNOWLEDGMENTS

We acknowledge resources provided by the USDA-ARS and the Donald Danforth Plant Science Center Proteomics and Mass Spectrometry Facility as well as the Minnesota Supercomputing Institute and funding support from the National Science Foundation (NSF) (Grant NSF/MCB-1042335, EF-1105249), and Office of Naval Research (ONR) (Grant N000141310552). The authors gratefully acknowledge the technical advice of Dr. Alexander Makarov, Thermo Fisher Scientific, and thank him for communicating a relationship approximating ion counts from signal to noise readings. Dr. Andre d'Avignon (High Resolution NMR Facility, Department of Chemistry, Washington University in St Louis) is acknowledged for help with NMR analysis. Any product or trademark mentioned here does not imply a warranty, guarantee, or endorsement by the authors or their affiliations over other suitable products.

REFERENCES

(1) Shewmaker, C. K.; Sheehy, J. A.; Daley, M.; Colburn, S.; Ke, D. Y. *Plant J.* **1999**, *20*, 401−412.
(2) Nawrath, C.; Poirier, Y.; Somerville, C. *Proc. Natl. Acad. Sci. U.S.A.* **1994**, *91*, 12760−12764.
(3) Kruger, N. J.; Masakapalli, S. K.; Ratcliffe, R. G. *J. Exp. Bot.* **2012**, *63*, 2309−2323.
(4) O'Grady, J.; Schwender, J.; Shachar-Hill, Y.; Morgan, J. A. *J. Exp. Bot.* **2012**, *63*, 2293−308.
(5) Fernie, A. R.; Morgan, J. A. *Plant, Cell Environ.* **2013**, *36*, 1738.
(6) Chen, X.; Shachar-Hill, Y. *J. Exp. Bot.* **2012**, *63*, 2343−2351.
(7) Heinig, U.; Gutensohn, M.; Dudareva, N.; Aharoni, A. *Curr. Opin. Biotechnol.* **2013**, *24*, 239−46.
(8) Libourel, I. G.; Gehan, J. P.; Shachar-Hill, Y. *Phytochemistry* **2007**, *68*, 2211−21.
(9) Libourel, I. G.; Shachar-Hill, Y. *Annu. Rev. Plant Biol.* **2008**, *59*, 625−50.
(10) Allen, D. K.; Libourel, I. G. L.; Shachar-Hill, Y. *Plant, Cell Environ.* **2009**, *32*, 1241−1257.
(11) Allen, D. K.; Shachar-Hill, Y.; Ohlrogge, J. B. *Phytochemistry* **2007**, *68*, 2197−2210.
(12) Sriram, G.; Fulton, D. B.; Shanks, J. V. *Phytochemistry* **2007**, *68*, 2243−2257.
(13) Wahrheit, J.; Nicolae, A.; Heinzle, E. *Biotechnol. J.* **2011**, *6*, 1071−1085.
(14) Zamboni, N. *Curr. Opin. Biotechnol.* **2011**, *22*, 103−108.
(15) Kruger, N. J.; Ratcliffe, R. G. *Biochimie* **2009**, *91*, 697−702.
(16) Stitt, M. *Curr. Opin. Plant Biol.* **2013**, *16*, 381−8.
(17) Sweetlove, L. J.; Fernie, A. R. *Annu. Rev. Plant Biol.* **2013**, *64*, 723−746.
(18) Nargund, S.; Sriram, G. *Mol. Biosyst.* **2013**, *9*, 99−112.
(19) Allen, D. K.; Laclair, R. W.; Ohlrogge, J. B.; Shachar-Hill, Y. *Plant, Cell Environ.* **2012**, *35*, 1232−1244.
(20) Mandy, D.; Goldford, J. E.; Yang, H.; Allen, D. K.; Libourel, I. G. L. *Plant J.* **2014**, *77*, 476−486.

(21) Olsen, J. V.; de Godoy, L. M. F.; Li, G.; Macek, B.; Mortensen, P.; Pesch, R.; Makarov, A.; Lange, O.; Horning, S.; Mann, M. *Mol. Cell. Proteomics* **2005**, *4*, 2010−2021.
(22) Mann, M.; Kelleher, N. L. *Proc. Natl. Acad. Sci. U.S.A.* **2008**, *105*, 18132−18138.
(23) Ong, S. E.; Blagoev, B.; Kratchmarova, I.; Kristensen, D. B.; Steen, H.; Pandey, A.; Mann, M. *Mol. Cell. Proteomics* **2002**, *1*, 376−386.
(24) Mann, M. *Nat. Rev. Mol. Cell Biol.* **2006**, *7*, 952−958.
(25) Ross, P. L.; Huang, Y. N.; Marchese, J. N.; Williamson, B.; Parker, K.; Hattan, S.; Khainovski, N.; Pillai, S.; Dey, S.; Daniels, S.; Purkayastha, S.; Juhasz, P.; Martin, S.; Bartlet-Jones, M.; He, F.; Jacobson, A.; Pappin, D. J. *Mol. Cell. Proteomics* **2004**, *3*, 1154−1169.
(26) Jehmlich, N.; Kopinke, F. D.; Lenhard, S.; Vogt, C.; Herbst, F. A.; Seifert, J.; Lissner, U.; Völker, U.; Schmidt, F.; Von Bergen, M. *Proteomics* **2012**, *12*, 37−42.
(27) Gygi, S. P.; Rist, B.; Gerber, S. A.; Turecek, F.; Gelb, M. H.; Aebersold, R. *Nat. Biotechnol.* **1999**, *17*, 994−999.
(28) Herbst, F. A.; Taubert, M.; Jehmlich, N.; Behr, T.; Schmidt, F.; Von Bergen, M.; Seifert, J. *Mol. Cell. Proteomics* **2013**, *12*, 2060−2069.
(29) Gevaert, K.; Impens, F.; Ghesquière, B.; Van Damme, P.; Lambrechts, A.; Vandekerckhove, J. *Proteomics* **2008**, *8*, 4873−4885.
(30) Ong, S. E. *Anal. Bioanal. Chem.* **2012**, *404*, 967−976.
(31) Evans, C.; Noirel, J.; Ow, S. Y.; Salim, M.; Pereira-Medrano, A. G.; Couto, N.; Pandhal, J.; Smith, D.; Pham, T. K.; Karunakaran, E.; Zou, X.; Biggs, C. A.; Wright, P. C. *Anal. Bioanal. Chem.* **2012**, *404*, 1011−1027.
(32) Bantscheff, M.; Schirle, M.; Sweetman, G.; Rick, J.; Kuster, B. *Anal. Bioanal. Chem.* **2007**, *389*, 1017−1031.
(33) Martin, S. F.; Munagapati, V. S.; Salvo-Chirnside, E.; Kerr, L. E.; Le Bihan, T. *J. Proteome Res.* **2012**, *11*, 476−86.
(34) Nelson, C. J.; Li, L.; Jacoby, R. P.; Millar, A. H. *J. Proteome Res.* **2013**, *12*, 3449−3459.
(35) Hughes, C.; Krijgsveld, J. *Trends Biotechnol.* **2012**, *30*, 668−76.
(36) Taubert, M.; Jehmlich, N.; Vogt, C.; Richnow, H. H.; Schmidt, F.; von Bergen, M.; Seifert, J. *Proteomics* **2011**, *11*, 2265−74.
(37) Jehmlich, N.; Schmidt, F.; Taubert, M.; Seifert, J.; Bastida, F.; von Bergen, M.; Richnow, H. H.; Vogt, C. *Nat. Protoc.* **2010**, *5*, 1957−66.
(38) Ullmann-Zeunert, L.; Muck, A.; Wielsch, N.; Hufsky, F.; Stanton, M. A.; Bartram, S.; Bocker, S.; Baldwin, I. T.; Groten, K.; Svatos, A. *J. Proteome Res.* **2012**, *11*, 4947−60.
(39) Marco-Urrea, E.; Seifert, J.; von Bergen, M.; Adrian, L. *J. Bacteriol.* **2012**, *194*, 4169−77.
(40) Blank, L. M.; Desphande, R. R.; Schmid, A.; Hayen, H. *Anal. Bioanal. Chem.* **2012**, *403*, 2291−305.
(41) Xu, Y.; Heilier, J. F.; Madalinski, G.; Genin, E.; Ezan, E.; Tabet, J. C.; Junot, C. *Anal. Chem.* **2010**, *82*, 5490−5501.
(42) Weber, R. J.; Southam, A. D.; Sommer, U.; Viant, M. R. *Anal. Chem.* **2011**, *83*, 3737−43.
(43) Southam, A. D.; Payne, T. G.; Cooper, H. J.; Arvanitis, T. N.; Viant, M. R. *Anal. Chem.* **2007**, *79*, 4595−602.
(44) Allen, D. K.; Young, J. D. *Plant Physiol.* **2013**, *161*, 1458−75.
(45) Hsu, F. C.; Obendorf, R. L. *Plant Sci. Lett.* **1982**, *27*, 129−135.
(46) Thompson, J. F.; Madison, J. T.; Muenster, A. M. E. *Ann. Bot.* **1977**, *41*, 29−39.
(47) Searle, B. C. *Proteomics* **2010**, *10*, 1265−9.
(48) Keller, A.; Nesvizhskii, A. I.; Kolker, E.; Aebersold, R. *Anal. Chem.* **2002**, *74*, 5383−92.
(49) Allen, D. K.; Ohlrogge, J. B.; Shachar-Hill, Y. *Plant J.* **2009**, *58*, 220−234.
(50) Krishnan, H. B.; Natarajan, S. S.; Mahmoud, A. A.; Nelson, R. L. *J. Agric. Food Chem.* **2007**, *55*, 1839−45.
(51) Berglund, M.; Wieser, M. E. *Pure Appl. Chem.* **2011**, *83*, 397−410.
(52) Lundell, N.; Schreitmuller, T. *Anal. Biochem.* **1999**, *266*, 31−47.
(53) Kaufmann, A.; Walker, S. *Rapid Commun. Mass Spectrom.* **2012**, *26*, 1081−90.
(54) Makarov, A. (Thermo Fisher Scientific). Personal communication, 2013.
(55) Masakapalli, S. K.; Kruger, N. J.; Ratcliffe, R. G. *Plant J.* **2013**, *74*, 569−82.
(56) Lonien, J.; Schwender, J. *Plant Physiol.* **2009**, *151*, 1617−1634.